Journal of Molecular Graphics and Modelling 53 (2014) 168–178

Contents lists available at ScienceDirect

Journal of Molecular Graphics and Modelling

journal homepage: www.elsevier.com/locate/JMGM

Probing the structural and electronic properties of small aluminum dideuteride clusters

Peng Shao[a,**], Xiao-Yu Kuang[b,*], Li-Ping Ding[b], Ming-Min Zhong[b], Ya-Ru Zhao[c]

[a] College of Science, Shaanxi University of Science & Technology, Xian 710021, China
[b] Institute of Atomic and Molecular Physics, Sichuan University, Chengdu 610065, China
[c] Department of Physics and Information Technology, Baoji University of Arts and Sciences, Baoji 721016, China

ARTICLE INFO

Article history:
Accepted 30 July 2014
Available online 7 August 2014

Keywords:
Density functional theory
Photoelectron spectra
Aluminum dideuteride clusters
Infrared spectra
Electronic properties

ABSTRACT

Adsorption of deuterium on the neutral and anionic Al_n^{λ} ($n = 1$–9, 13; $\lambda = 0, -1$) clusters has been investigated systematically using density functional theory. The comparisons between the Franck–Condon factor simulated spectra and the measured photoelectron spectroscopy (PES) of Cui and co-workers help to search for the ground-state structures. The results showed that D_2 molecule tends to be dissociated on aluminum clusters and forms the radial Al—D bond with one aluminum atom. By studying the evolution of the binding energies, second difference energies and HOMO–LUMO gaps as a function of cluster size, we found Al_2D_2, Al_6D_2 and $Al_7D_2^-$ clusters have the stronger relative stability and enhanced chemical stability. Also, considering the larger adsorption energies of these three clusters, we surmised that Al_2, Al_6 and Al_7^- may be the better candidates for dissociative adsorption of D_2 molecule among the clusters we studied. Furthermore, the natural population analysis (NPA) and difference electron density were performed and discussed to probe into the localization of the charges and reliable charge-transfer information in Al_nD_2 and $Al_nD_2^-$ clusters.

1. Introduction

Molecular, semiconductor and atomic clusters in the nanometer size range are a current topic of research. In particular, atomic clusters have been an interesting subject not only because they can form building blocks of a novel class of cluster assembled materials [1], but also an understanding of their stabilities has great scientific significance.

Nano-assemblies of light metal clusters have potential applications in hydrogen energy production technology, which is a safe, compact and inexpensive system able to store a large amount of hydrogen. Among them, aluminum clusters [2–5] are the most studied system. Because it is a common and cheap metal with lighter mass compared with precious hydrogen-absorbing metal, such as palladium [6] and platinum. The electronic structure of aluminum is free-electronlike just as the alkali metal. The electronic structure of alkali metal clusters has been successfully described by the jellium model [7,8]. So it is expected that aluminum clusters can also be studied by applying this simple model. The so-called jellium model predicts that clusters with closed-shell electronic configurations are particularly stable. Thus, clusters with 2, 8, 20, 40... electrons can close $1s^2, 1p^6, 1d^{10}, 2s^2, 1f^{14}, 2p^6$... shells, and should be very stable. In the case of aluminum clusters, Al_7^+ and Al_{13}^- clusters containing 20 and 40 electrons, respectively, are known to be stable [9]. Furthermore, Al_7 and Al_{13} are also tested to be particularly stable [10,11] because their valence electronic configurations approach closed-shell magic configurations, as characterized by the jellium model. However, several other experimental and theoretical studies [12,13] indicate that small aluminum clusters do not comply with this well-known jellium model. Compared with alkali metal clusters, the two important issues for aluminum clusters are that: the lack of *s* and *p* bands overlap and large perturbations due to +3 ionic cores. Al atom has $3s^23p^1$ configuration and the *s* and *p* orbitals are separated by an energy gap of 4.99 eV. So the *s*–*p* overlap [14,15] is very small in small Al clusters and aluminum may behave as a monovalent atom. According to these, it is believed it is only when the full *s*–*p* mixing is achieved that aluminum can be considered to be trivalent, and then it is expected the jellium model begins to work. The electronic structure of aluminum clusters is still unclear and controversial.

Hydrogenated and dehydrogenated aluminum clusters are interesting as candidates for hydrogen-absorbing nanomaterial [16,17]. It has been proposed that the adsorption of hydrogen on

* Corresponding author at: Tel.: +86 28 85405515; fax: +86 28 85405515.
** Corresponding author.
E-mail addresses: scu_sp@163.com (P. Shao), scu_yp@163.com (X.-Y. Kuang).

http://dx.doi.org/10.1016/j.jmgm.2014.07.016
1093-3263/

Table 1
Experimental adiabatic detachment energies (ADE) of Al_n^{λ} and $Al_nD_2^{\lambda}$ (n = 2–9, 13; λ = 0, −1) compared to those calculated for the ground-state isomers.

N	ADE (eV)									
	Al_n^-				$Al_nD_2^-$					
	Exp.[a]	**Exp.**[b]	B3PW91	PW91	**Exp.**[c]	B3PW91	PW91	B3LYP	HF	MP2
2	1.46 ± 0.01		1.52	1.56		1.42	1.39	1.30	0.77	1.16
3	1.89 ± 0.04	1.53	1.59	1.75	1.90 ± 0.10	1.79	1.86	1.73	0.72	1.83
4	2.20 ± 0.05	1.74	2.14	2.12		1.95	1.95	1.81	1.50	1.63
5	2.25 ± 0.05	1.82	2.10	2.08		2.06	2.11	2.00	1.02	1.00
6	2.63 ± 0.06	2.09	2.50	2.49	1.66 ± 0.15	1.87	1.81	1.79	1.76	1.44
7	2.43 ± 0.06	1.96	2.09	2.12	2.95 ± 0.04	2.90	2.89	2.79	1.72	3.38
8	2.35 ± 0.08	2.22	2.25	2.17	2.27 ± 0.04	2.28	2.35	2.17	1.68	1.62
9	2.85 ± 0.08	2.47	2.59	2.63	2.91 ± 0.04	2.38	2.40	2.36	1.24	3.38
13	3.62 ± 0.06	2.86	3.39	3.36	3.64 ± 0.08	3.49	3.46	3.33	2.58	2.52

[a] Ref. [41].
[b] Ref. [42].
[c] Ref. [33].

Al_{13} can provide an electron to complete its electronic configuration, therefore $Al_{13}H$ may be suitable for the preparation of new cluster-assembled materials [18–21]. However, some early theoretical [22,23] and experimental [24] studies indicate that aluminum has a poor metal surface for dissociative adsorption of H_2. In other words, it cannot adsorb molecular hydrogen under normal condition, and there is a large activation energy barrier (≥0.5 eV) [23] for dissociation of H_2. Therefore, it is very interesting to study the interaction between H_2 and aluminum clusters, which are expected to have different properties from the bulk surface.

An early research to understand hydrogen interaction with aluminum clusters was made by Upton [25,26]. Their results suggested that Al_6 is the smallest cluster that will adsorb H_2. Cox et al. [27] found that chemisorption of D_2 on neutral Al clusters is relatively slow and strongly size specific, with only Al_6 and Al_7 exhibiting significant reactivity. Very recently, Henry and co-workers have investigated the interaction of hydrogen with aluminum clusters, including the binding of H atoms to Al_{12} and doped $Al_{12}X$ (X = Mg, Al, Si) clusters [28–31]. Reaction profiles for the formation of $(Al_{13})_2$ dimers from a range of cluster and H atom combinations were also determined by them [32]. Cui et al. [33] investigated $Al_nD_2^-$ (n = 3, 6–15) anions using photoelectron spectroscopy, which can reveal the nature of the interaction between D_2 and the Al_n^- clusters. Their results suggested that for the closed-shell Al_n^- (n = 9, 11, 13, and 15), D_2 is physisorbed on the clusters; whereas for the open-shell Al_n^- (n = 8, 12 and 14), D_2 is chemisorbed on the clusters; for $Al_nD_2^-$ (n = 3, 6, 7, and 10), their PES spectra are totally different from those of the corresponding bare Al_n^- cluster, which suggested that D_2 is likely to be dissociatively adsorbed onto the clusters. In their experiment, D_2 is used instead of H_2 for better mass resolution. In theoretical calculations, the formation energies and electronic structure of D–Al and H–Al bonds are identical; however, the vibration states in the anharmonic D–Al potential are closer to each other than for H–Al. On the other hand, the zero-point energies, reduced masses, and IR intensities are unequal. Therefore, to gain insight into the electronic properties of aluminum clusters and offer more information for studying the interaction between molecular deuterium and aluminum clusters, we report a more extensive and systematic density functional theory investigation on the small sized neutral and anionic Al_n and $Al_nD_2^{\lambda}$ (n = 1–9, 13; λ = 0, −1) clusters. The main objective of this research is to investigate the nature of interaction between molecular deuterium and small neutral and anionic aluminum clusters, meanwhile, to compare our extensive computational results with previously experimental findings [33]. The various ground-state minimum structures for each sized clusters are also obtained.

2. Computational methods

Geometrical structure optimizations and frequency analysis of $Al_nD_2^{\lambda}$ (n = 1–9, 13; λ = 0, −1) clusters were performed by density functional theory (DFT) method using the GAUSSIAN 03 program [34]. Becke's hybrid three-parameter functional combined with Perdew–Wang's correlation functional (B3PW91) [35–38] were employed for studying the bare aluminum clusters and aluminum dideuteride clusters. Due to the aluminum atom has an unoccupied *d* orbital, it is necessary to describe aluminum systems which have high valence with using *d* functions in the basis set. As previously shown, an all-electron basis set with the addition of *d* functions is essential for a proper description of high-valence Al atoms [22]. We chose the triple-ξ basis set 6-311+G(2d, 2p) [39,40], which include a *d*-type polarization function on heavy atoms and a *p*-type polarization function on deuterium, for our systems. Moreover, the reliability of current computational method was tested by comparing calculated adiabatic detachment energies (ADEs) using several exchange-correlation DFT functionals, Hartree–Fock and MP2 method. The results comparing with experimental values [33,41,42] are presented in Table 1.

To search for the lowest energy structure of aluminum dideuteride clusters, the equilibrium geometries of bare aluminum clusters were first studied. The pure aluminum clusters in the range of 2–13 atoms have been well studied [8,15,43–46]. We searched the pure neutral and anionic aluminum clusters by considering all the possible structures reported in previous papers. Then the adsorption models of one D_2 molecule or two D atoms on the lowest energy Al_n and Al_n^- clusters were firstly built. According to earlier investigation [47], we considered not only the most stable structures of the pure clusters but also their other low-energy isomers during the adsorption addition, since the adsorption stabilities of the latter may be competitive with or even exceed that of the most stable conformations. Almost all the possible adsorption sites have been considered. Furthermore, the previous studies on the structure of Al—H and Al—O system are also employed as a guide [25,48,21,49–57].

All the initial structures are first optimized at B3PW91/6-311+G(2d, 2p) level. Afterwards, a selected set of the low-energy optimized structures was tested by PW91PW91 [34] and B3LYP [35,58] functional. Due to the spin polarization, every initial structure is optimized at various possible spin multiplicities. It is worth pointing out that all of the adsorption clusters are found to prefer the lowest spin state. In order to confirm that the optimized geometry corresponds to a local minimum in potential energy, each of them is followed by an analysis of harmonic vibrational frequencies. Three criteria are consulted in comparing the theoretical results with the experimental data to select most likely candidate structures: (1) the

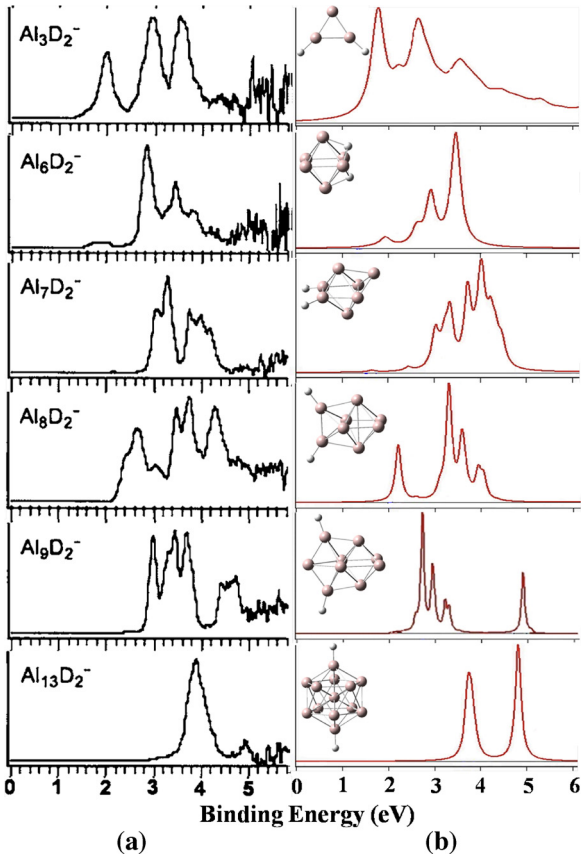

Fig. 1. (a) Photoelectron spectra of $Al_nD_2^-$ (n = 3, 6–9, 13) measured at 193 nm (6.424 eV). (The spectra are taken from Ref. [33]. Copyright 2006 American Institute of Physics) (b) Simulated photoelectron spectra for the lowest-energy structures of $Al_nD_2^-$ (n = 3, 6–9, 13) clusters at the B3PW91/6-311++G (2d, 2p) level.

relative energies; (2) the adiabatic detachment energies (ADEs); (3) the number of distinct peaks of simulated photoelectron spectra in the low-binding-energy range of ≤4 eV and their relative positions.

3. Results and discussion

3.1. Comparison of theoretical simulation and experimental photoelectron spectra

A PES experiment on $Al_nD_2^-$ (n = 3, 6–15) was carried out using a magnetic-bottle time-of-flight photoelectron spectrometer equipped with a laser vaporization cluster source by Wang's group [33]. Well-resolved PES spectra serve as electronic "fingerprints" of the underlying clusters and can be used for comparisons with theoretical simulations. In this case, we have performed the simulated spectra in framework of the Franck–Condon (FC) approximations [59,60] for $Al_nD_2^-$ (n = 3, 6–15) isomers at B3PW91/6-311++G (2d, 2p) theory level. In this fashion, the Franck–Condon factors were derived for a progression of up to 20 quanta. Then the computed FCFs were used to simulate the vibrational structure of neutral to anion state photo-detachment spectrum, employing a Gaussian line-shape for each vibration component. Due to the nonadiabatic interactions and anharmonic resonances are not included during the Franck–Condon factor calculations, it is not possible to quantitatively compare calculated intensities with experimental ones, but the positions and the general shape of the peaks overall agree with experimental spectra. The PES data at photon energy 193 nm (6.424 eV) for $Al_nD_2^-$ (n = 3, 6–9, 13) clusters are presented in Fig. 1(a), and the results of Franck–Condon simulation for the ground-state isomers are shown in Fig. 1(b). As shown in Fig. 1, the numbers of distinct peaks of simulated photoelectron spectra in the low-binding-energy range of ≤4 eV and their relative positions overall agree with the experimental spectra. Those increase the confidence in the reliability of the ground-state structures isomers obtained. Additionally, simulated PES from top two low-lying anion structures were also presented in supplementary material (Fig. S3).

3.2. Geometrical structures

The starting point is their geometrical structures for any description of cluster properties. Based on the method that has been pointed out above, a large number of optimized isomers for $Al_nD_2^\lambda$ (n = 1–9, 13; λ = 0, −1) clusters are obtained. In order to keep the length of our paper, we only discuss the geometries corresponding to the ground-state. We believe that we have identified the geometrical structures of small size bare aluminum clusters and aluminum dideuteride clusters correctly. This belief is based on our ability to explain the adiabatic detachment energies and infrared spectra quantitatively. The ground-state geometries of neutral and anionic Al_nD_2 and Al_n clusters, which containing 2–6 and 7–9, 13 aluminum atoms, were optimized at the B3PW91/6-311++G (2d, 2p) level and presented in Figs. 2 and 3, respectively. Their corresponding electronic states, symmetries, HOMO energies, LUMO energies, HOMO–LUMO gaps and the vibration frequencies with the most IR intensities are summarized in Table 2. In addition, some low-lying isomers for each size together with their information are listed in supplementary material (Figs. S1 and S2).

3.2.1. Bare aluminum clusters Al_n (n = 1–9, 13; λ = 0, −1)

Aluminum is a typical metal with deficient metallic bonding, which may lead to the structure with large average number of first nearest neighbors and high symmetry. As shown in Table 2, almost all the neutral and anionic aluminum clusters have high symmetry, which has been pointed out in previous reports [8,15,43–46]. The ground state of Al_2 is calculated to be $^3\prod_u$ with a bond length of 2.74 Å. For Al_2^-, the ground state is $^4\sum_g^-$ with a bond length of 2.56 Å. These results are in good agreement with Zhan's studies [61] who determined its ground state as $^3\prod_u$ and two excited states ($^3\sum_g^-$ and $^1\sum_g^+$) at CCSD (T)/aug-cc-pVxZ (x) D, T, Q) level. The ground-state structures of Al_n change from planar to three-dimensional (3D) structure at n = 6, while this transition occurs at n = 5 for anionic clusters. The Al_5^- cluster looks like a planar structure. But if you take a good look at Fig. 2, you will find it is a 3D structure. All the ground-state structures of neutral clusters are very similar to their corresponding anions. Al_{13} is a classic example for studying the relative stability of icosahedral structures, and it has been well studied [15,19,20,46]. Our ground-state of the 13-atom aluminum cluster is a Jahn-Teller distorted icosahedron with D_{3d} symmetry, which is in accord with the result obtained by Fournier [46]. The clusters consist of two atomic shells, and the inner one being just one aluminum atom. In order to make sure the optimized structure is a local minimum or transition state on the potential energy surface, we calculated the vibrational spectra for Al_{13} and Al_{13}^-. It will be discussed in the next part.

3.2.2. $Al_nD_2^\lambda$ (n = 1–9, 13; λ = 0, −1) clusters

We present the ground-state structures of $Al_nD_2^\lambda$ (n = 2–9, 13; λ = 0, −1) in Figs. 2 and 3. Firstly, we discuss the general features observed in these clusters. The small size Al_nD_2 clusters favor planar structures for n = 3, 5 and three-dimensional (3D) structures for n = 2, 4, 6–9, 13; while for the anionic clusters, only $Al_3D_2^-$ and $Al_4D_2^-$ tend to be planar structures. Most of the ground-state

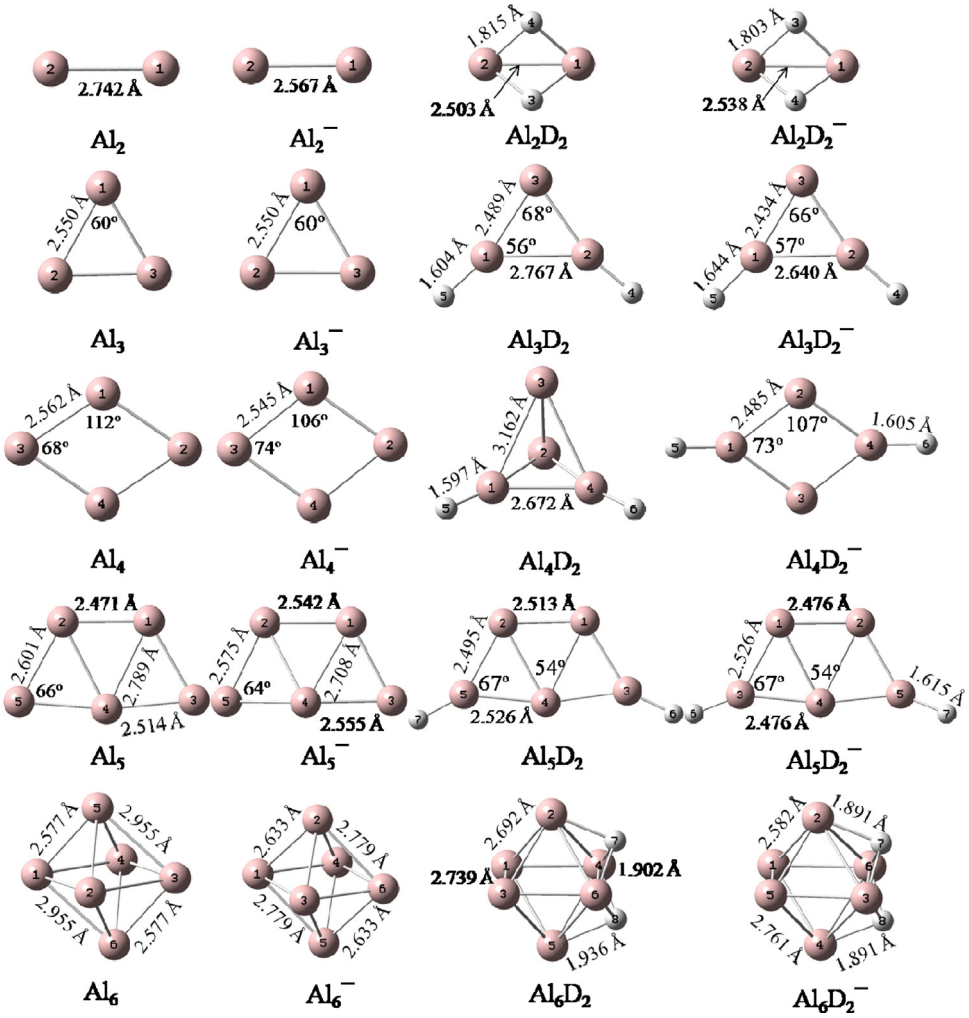

Fig. 2. The ground-state structures of Al_n^{λ} and $Al_nD_2^{\lambda}$ ($n = 2$–6; $\lambda = 0, -1$) clusters.

adsorption clusters can be obtained by adsorbing two deuterium atoms on the lowest energy bare aluminum clusters, but the ground-state Al_4D_2, Al_8D_2 and $Al_8D_2^-$ clusters generate from the corresponding low-energy aluminum isomers. In this case, the neutral and anionic $Al_nD_2^{0/-}$ clusters have the similar structures except for $n = 4$ and 8. The deuterium atom which adsorbed on the surface of aluminum clusters tends to radial bound to a single Al atom. Only when $n = 2$ and 6, the D atoms are edge-capped and face-capped on the aluminum clusters, respectively. The adsorption of two deuterium atoms in D_2 molecular form is also considered by us. However, the deuterium molecule dissociates for most of the clusters according to our calculation. The D_2 molecule dissociation may be catalyzed by the presence of small aluminum clusters with special properties with respect to surfaces. Only few isomers with D_2 molecular adsorption are obtained in our calculation. They are significantly higher in total energy and cannot be selected as the ground-state structure. So we show some of them (e.g. isomer 2N-e, 7N-e and 2A-d) in supplementary material (Figs. S1 and S2).

As seen from the Fig. 2, both Al_2D_2 and $Al_2D_2^-$ can be obtained by capping deuterium atoms on the bridge sites of aluminum dimer, thus they have the same C_{2v} symmetry. The ground-state structures of Al_3D_2, $Al_3D_2^-$, $Al_4D_2^-$ and Al_5D_2 are optimized as planar structure, and they have $^2B_1$, $^1A_1$, ^2A_g and $^2A_1$ electronic state, respectively. For $Al_6D_2^{0/-}$, the anionic isomer is derived from the neutral ground state. Its ADE is 1.87 eV which agree well with the experimental values (1.66 ± 0.15 eV) [33]. Actually, another anionic isomer (6A-a) listed in the supplementary material (Fig. S1) is 0.48 eV lower in total energy than the one we show here. In 6A-a isomer, two deuterium atoms bind in to opposite Al atoms. The ADE of this isomer is calculated to be 2.67 eV. If 6A-a isomer is observed as the ground state isomer, there will be a huge difference between the calculated and experimental values (1.66 ± 0.15 eV) [33]. On the other hand, there are two half filled 1*d* orbital on Al_6 whose lobes are extending from 3-fold sites and deuterium atoms on opposite site can interact only one orbital. However, deuterium atoms on 3-fold sites can interact with both orbital and make closed 2*s* and 1*d* shells. In this case, we choose the face-capped isomer as the ground-state structure. Starting at $n = 7$, deuterium atoms in the lowest-energy structures of $Al_nD_2^{0/-}$ tend to D binds in to a single Al atom. In the radial position, deuterium atom would form a covalent bond with the Al atom; while in the bridge or face bonded case, deuterium's electron would become delocalized. We believe that the various types of Al–D bonds can be utilized to design $Al_nD_2^{0/-}$ clusters with different properties. Kiran and co-workers [50] have performed an in-depth research about the types of Al–H bonds and proposed a rule for magic Al_nD_m clusters. Firstly, they put forward a hypothesis as that: when H atom is bound in to a single Al atom, the Al–H pair can only donate 2 electrons as two of the four valence electrons of the Al–H pair are localized in the covalent bond; when H atom is bound to two or more Al atoms, each H and Al atom can donate 1 and 3 electrons, respectively. On the basis of jellium model, they gave an equation for magic $Al_nH_m \rightarrow Al_{n-i}(AlH)_iH_{m-i}$ clusters as

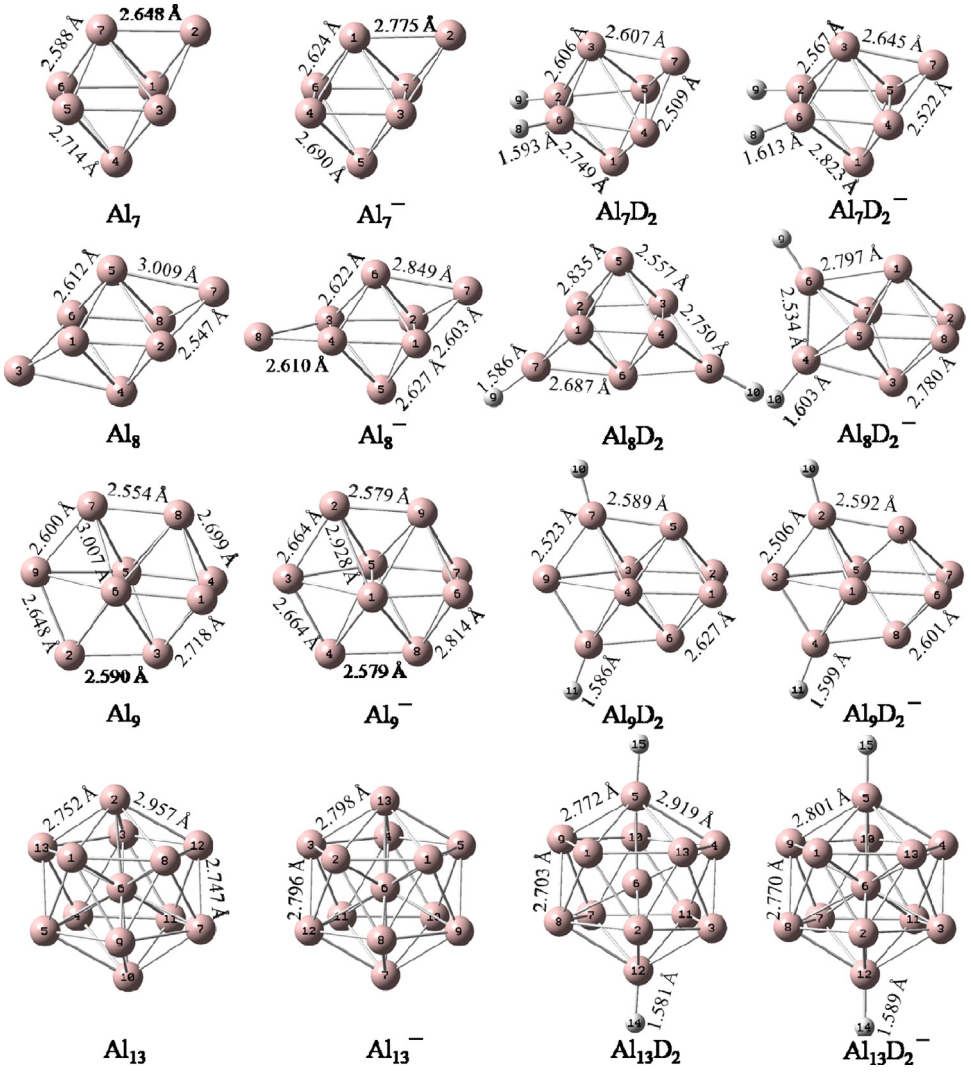

Fig. 3. The ground-state structures of Al_n^{λ} and $Al_nD_2^{\lambda}$ (n = 7–9, 13; λ = 0, −1) clusters.

following: $N = 3(n\text{-}i) + (m\text{-}i) = 3n\text{-}2i + m$, $i \le n$ and $i \le m$. Note that i is the number of radial bounded H atoms and N is the total number of valence electrons. However, we think this equation still need to be tested and verified, and further studies on the types of Al–H bonds are still necessary.

For $Al_{13}D_2$ cluster, we considered icosahedral isomers with two deuterium atoms on the top, bridge, or hollow site. The results show that both of the neutral and anionic $Al_{13}D_2$ clusters with deuterium atoms adsorbed on the top site are optimized as the most stable isomer, while they have the different symmetry (C_{2h} and D_{5d}). To provide a spectroscopic fingerprint to assist experimentalists to distinguish between different species and different isomers, the infrared spectra for Al_{13}, Al_{13}^-, $Al_{13}D_2$ and $Al_{13}D_2^-$ were calculated, and the results are presented in Fig. 4. The spectrum for Al_{13} has four dominant peaks, which is in line with the result obtained by Henry and co-workers [62]. The highest intensity peak, located at 181 cm^{-1}, is associated with symmetrical stretching in pairs of surface atoms on opposite sides of the cluster. The spectrum for Al_{13}^- has only two peaks, and the highest intensity peak located at 172 cm^{-1}. The features of anionic Al_{13}^- cluster are different from those of neutral one, which may be due to that the former has the higher symmetry (I_h) than the latter (D_{3d}). With regard to the $Al_{13}D_2$ and $Al_{13}D_2^-$ clusters, the most intense peaks in these spectra are generally associated with the vibrational motion of the D atoms and located at 1389 cm^{-1} and 1355 cm^{-1}, respectively. Vibrational motions of Al atoms are found in the far-infrared region (100–400 cm^{-1}) which is in accord with those observed in pure $Al_n^{0/-}$ clusters. However, due to the symmetric Al–Al stretching, the most intense peaks in this region show only slight shifts relative to the corresponding vibration in the pure aluminum cluster. The complex nature of the far-infrared region when combined with the characteristic Al–D stretches can be used as a fingerprint for identifying the different $Al_{13}D_2$ isomers.

3.3. Relative stabilities and adsorption energy

The second difference energies ($\Delta_2E(n)$), which can be compared with the relative abundances determined in mass spectroscopy experiment, are a quite sensitive quantity that reflects the relative stability of clusters [63]. Thus we have calculated the $E_b(n)$ and $\Delta_2E(n)$ to determine the relative stabilities of the most stable Al_n^{λ} and $Al_nD_2^{\lambda}$ (n = 1–9, 13; λ = 0, −1) clusters. For $Al_nD_2^{\lambda}$ (λ = 0, −1) clusters, $E_b(n)$ and $\Delta_2E(n)$ are defined as the following formula:

$$E_b(n) = \frac{nE(\mathrm{Al}) + E(\mathrm{D}) + E(\mathrm{D}^{\lambda}) - E(\mathrm{Al}_n\mathrm{D}_1^{\lambda})}{n+2}, \quad (1)$$

$$\Delta_2E(n) = E(\mathrm{Al}_{n-1}\mathrm{D}_2^{\lambda}) + E(\mathrm{Al}_{n+1}\mathrm{D}_2^{\lambda}) - 2E(\mathrm{Al}_n\mathrm{D}_2^{\lambda}), \quad (2)$$

Table 2
Electronic states, symmetries, HOMO energies, LUMO energies, HOMO–LUMO gaps (HL gap) and the vibration frequencies with most IR intensities of Al_n^{λ} and $Al_nD_2^{\lambda}$ (n = 2–9, 13; λ = 0, −1) clusters.

Isomer	State	Sym	HOMO (eV)	LUMO (eV)	HL gap (eV)	Frequency (cm^{-1})
Al_2^-	$^3\prod_u$	$D_{\infty h}$	−4.4107	−3.0512	1.3595	267
Al_2	$^4\sum_g$	$D_{\infty h}$	0.0596	2.1353	2.0757	320
$Al_2D_2^-$	^1A	C_{2v}	−5.8546	−3.1209	2.7337	243, 614, 686, 754, 884, 972
Al_2D_2	$^2A_1$	C_{2v}	0.2275	2.0945	1.8670	265, 526, 737, 781, 841, 960
Al_3^-	$^2A_1'$	D_{3h}	−4.7340	−3.1691	1.5649	223, 335
Al_3	$^1A_1'$	D_{3h}	−0.3167	1.2346	1.5513	225, 343
$Al_3D_2^-$	$^2B_1$	C_{2v}	−5.2698	−3.2738	1.9960	200, 207, 247, 345, 1326, 1324
Al_3D_2	$^1A_1$	C_{2v}	−0.2778	1.6547	1.9326	217, 228, 251, 400, 1216, 1226
Al_4^-	$^3B_{3g}$	D_{2h}	−4.9642	−3.6224	1.3418	50, 181, 217, 294, 308, 331
Al_4	^2A_g	D_{2h}	−0.6661	0.8359	1.5021	83, 155, 269, 271, 313, 331
$Al_4D_2^-$	$^1A'$	C_s	−4.7773	−2.8749	1.9023	130, 223, 233, 298, 1340, 1347
Al_4D_2	^2A_g	C_{2h}	−0.6841	0.9641	1.6482	28, 211, 263, 374, 417, 1312
Al_5^-	$^2B_2$	C_{2v}	−5.1212	−3.3283	1.7930	31, 117, 184, 258, 296, 388
Al_5	$^1A'$	C_s	−0.8515	0.5388	1.3902	74, 111, 253, 269, 360, 372
$Al_5D_2^-$	$^2A_1$	C_{2v}	−5.1465	−3.3707	1.7758	208, 249, 262, 409, 1365, 1368
Al_5D_2	^1A	C_2	−0.7927	0.8185	1.6112	202, 256, 306, 441, 1277, 1280
Al_6^-	$^1A_{1g}$	D_{3d}	−5.2546	−3.6254	1.6292	91, 121, 289
Al_6	$^2A_{1g}$	D_{4h}	−1.1802	0.2343	1.4145	82, 215, 278
$Al_6D_2^-$	$^1A'$	C_s	−5.4303	−3.0134	2.4169	248, 293, 318, 704, 742, 762
Al_6D_2	$^2A'$	C_s	−0.7320	0.8689	1.6008	225, 245, 282, 291, 523, 708
Al_7^-	$^2A_1$	C_{3v}	−4.8942	−3.0686	1.8256	39, 203, 227, 274, 301, 326
Al_7	$^1A_1$	C_{3v}	−1.0936	0.5404	1.6341	78, 216, 278, 294, 298,
$Al_7D_2^-$	^2A	C_1	−5.5294	−3.8001	1.7293	245, 285, 330, 349, 1344, 1360
Al_7D_2	$^1A'$	C_s	−1.7046	0.6389	2.3435	235, 304, 325, 349, 1279, 1287
Al_8^-	^1A_g	C_{2h}	−5.0761	−3.2251	1.8509	25, 198, 273, 292, 317, 382
Al_8	$^2A'$	C_s	0.2702	−1.2479	1.5181	230, 242, 255, 256, 293, 366
$Al_8D_2^-$	^1A	C_2	−4.8072	−3.0267	1.7805	153, 295, 329, 368, 1378, 1379
Al_8D_2	$^2B_1$	C_{2v}	−1.1249	0.2694	1.3943	51, 196, 226, 296, 1308. 1313
Al_9^-	$^2A'$	C_s	−5.1520	−3.5370	1.6150	167, 173, 188, 250, 325, 351
Al_9	^1A	C_2	−1.5785	−0.1170	1.4615	153, 174, 183, 199, 257, 304
$Al_9D_2^-$	$^2B_1$	C_{2v}	−4.9863	−3.4317	1.5546	141, 280, 319, 341, 1374, 1375
Al_9D_2	$^1A'$	C_s	−1.3176	0.1910	1.5086	108, 283, 295, 358, 1324, 1325
Al_{13}^-	$^2A_1$	D_{3d}	−5.6127	−4.2714	1.3412	106, 181, 190, 228, 271, 276
Al_{13}	$^1A_1$	I_h	−2.4346	0.2991	2.7337	171, 173, 378, 380
$Al_{13}D_2^-$	^2B_u	C_{2h}	−5.7666	−4.4156	1.3500	174, 188, 305, 335, 370, 1389
$Al_{13}D_2$	^1A_g	D_{5d}	−2.5358	0.2229	2.7486	161, 173, 247, 335, 402, 1355

where E(Al), E(D), $E(D^{\lambda})$, $E(Al_nD_2^{\lambda})$, $E(Al_{n-1}D_2^{\lambda})$ and $E(Al_{n+1}D_2^{\lambda})$ denote the total energies of the Al, D, D^{λ}, $Al_nD_2^{\lambda}$, $Al_{n-1}D_2^{\lambda}$ and $Al_{n+1}D_2^{\lambda}$ clusters, respectively.

For Al_n^{λ} (λ = 0, −1) clusters, $E_b(n)$ and $\Delta_2E(n)$ are defined as follows:

$$E_b(n) = \frac{(n-1)E(\mathrm{Al}) + E(\mathrm{Al}^{\lambda}) - E(\mathrm{Al}_n^{\lambda})}{n}, \quad (3)$$

$$\Delta_2E(n) = E(\mathrm{Al}_{n-1}^{\lambda}) + E(\mathrm{Al}_{n-1}^{\lambda}) - 2E(\mathrm{Al}_n^{\lambda}), \quad (4)$$

where E(Al), $E(Al^{\lambda})$, $E(Al_n^{\lambda})$, $E(Al_{n-1}^{\lambda})$ and $E(Al_{n+1}^{\lambda})$ denote the total energies of the Al, Al^{λ}, Al_n^{λ}, Al_{n-1}^{λ} and Al_{n+1}^{λ} clusters, respectively.

The $E_b(n)$ and $\Delta_2(E_n)$ values of the lowest energy Al_n^{λ} and $Al_nD_2^{\lambda}$ (n = 1–9; λ = 0, −1) clusters against the corresponding number of the Al atoms are plotted in Fig. 5. We can easily get the features of the size evolution from this figure. For pure Al_n and Al_n^- clusters, the binding energies gradually increase with the cluster size increasing. Their second difference energies exhibit a small odd-even alternation along with cluster size. Such behavior has been seen in previous studies [46]. A visible peak occurs at n = 7, which hints that the Al_7 and Al_7^- clusters are more stable than its neighboring clusters. We always expect the Al_7^+ exhibit pronounced stability as it has 20 electrons—enough for electronic shell closure of the $2s^2$ shell. But the Al_7 and Al_7^- clusters contain 21 and 22 electrons respectively, so they would not correspond to shell closure. A better explanation may be that the stability is associated not only with closed electronic shells (N_e = 20, 40), but also to a lesser extent, with numbers of electrons just above and below the shell closing numbers. Another possible explanation is that the number of bonds (number of nearest neighbor atom pairs) is larger in Al_7 and Al_7^- than in their neighbors, resulting in Al_7 and Al_7^- appear stable in the plot of second difference energies.

For Al_nD_2 and $Al_nD_2^-$ clusters, the binding energies per atom is higher than those of the corresponding size pure aluminum clusters, reflecting that the interactions between D atoms and Al_n supply additional energies to the total binding energies. In other words, the stability of $Al_nD_2^{0/-}$ clusters is enhanced when D atoms adsorbed on the pure $Al_n^{0/-}$ clusters. The two curves of binding energies for Al_nD_2 and $Al_nD_2^-$ clusters are smooth lines with very slight increasing. Just like the pure aluminum clusters, the second difference energies of adsorbed clusters also exhibit a small odd-even alternation phenomenon along with cluster size. The conspicuous peaks appear at Al_2D_2, Al_6D_2 and $Al_7D_2^-$, which is in accord with the features of binding energies. Those indicate that the three clusters are more stable than others. The Al_2D_2, Al_6D_2 and $Al_7D_2^-$ clusters have 8, 20 and 18 valence electrons respectively, so they satisfy the electronic shell closure requirement. According to the jellium model, it is easy to explain their higher stability. In addition, to further explain the stability of $Al_7D_2^-$ isomer, we against discusses the frontier orbital and electronic properties of it.

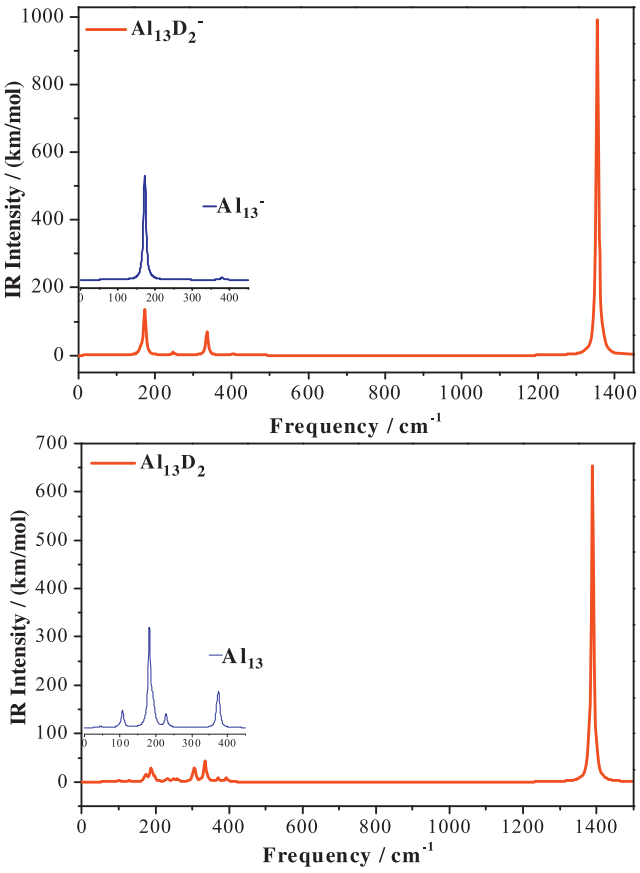

Fig. 4. Infrared spectra of $Al_{13}^{0/-}$ and $Al_{13}D_2^{0/-}$ clusters.

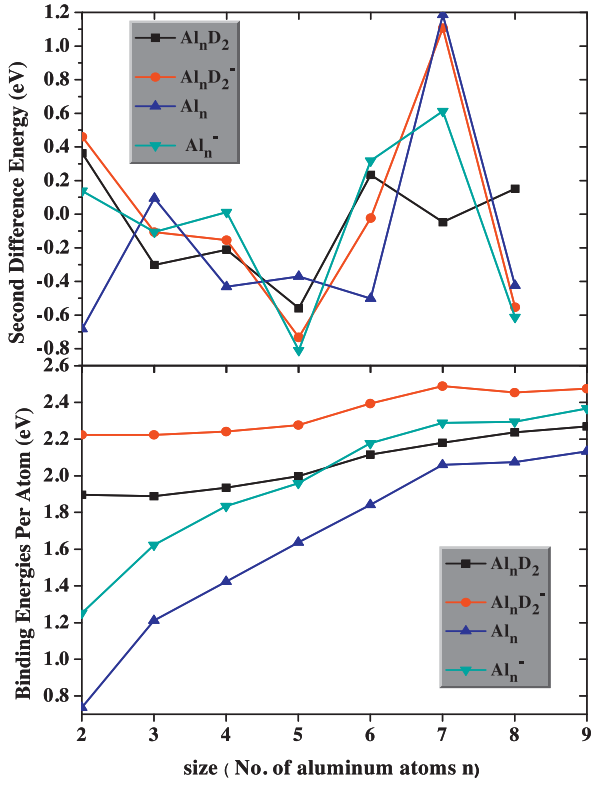

Fig. 5. Size dependence of the binding energies per atom $E_b(n)$, and the second difference energies $\Delta_2(E_n)$ for the ground-state structures of Al_n^{λ} and $Al_nD_2^{\lambda}$ (n = 2–9; λ = 0, −1) clusters.

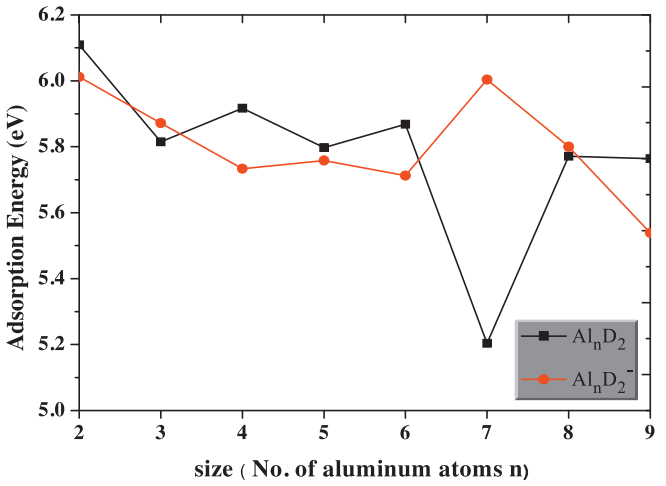

Fig. 6. The adsorption energy of two deuterium atoms on the pure neutral or anionic aluminum clusters as a function of clusters size.

The adsorption energies of two D atoms on neutral or anionic aluminum clusters are defined as the following formula:

$$E_{ads}(n) = E(Al_n^{\lambda}) + 2E(D) - E(Al_nD_2^{\lambda}), \quad (5)$$

where $E(Al_n^{\lambda})$, $E(D)$, and $E(Al_nD_2^{\lambda})$ denote the total energies of the Al^{λ}, D, and $Al_nD_2^{\lambda}$ clusters, respectively. The adsorption energies for the most stable configurations of $Al_nD_2^{\lambda}$ (n = 1–9; λ = 0, −1) as a function of n are plotted in Fig. 6. According to Fig. 6, it is found that the two curves show the odd-even alternation behavior, but the one for $Al_nD_2^-$ is irregular. This odd–even behavior has been seen in Al–H systems [48]. With regard to Al_nD_2 clusters, the clusters with even number of Al atoms have higher E_{ads} than the clusters with odd numbers. These imply that the adsorption of two D atoms would take place easier for Al_n clusters with even n. There is a minimum of Al_7D_2. However, upon an extra electron attachment, the adsorption energy represent a significantly increase, resulting in a more stable cluster $Al_7D_2^-$, which is also agreement with the large value of VDE compared with others. The other two conspicuous peaks appear at Al_2D_2 and $Al_2D_2^-$, suggesting they are more stable compared with other clusters. Those are in agreement with the above results of binding energy and second difference energy.

The binding energies per atom $E_b(n)$ for $Al_{13}^{0/-}$ and $Al_{13}D_2^{0/-}$ are also calculated. As mentioned above, Al_{13} has an almost spherical compact icosahedral structure and with its 39 valence electrons is lacking just one electron to complete its outer electronic shell. In principle, the Al_{13}^- anion should be more stable than the other anionic clusters. In agreement with this, our calculations showed that the ADE of Al_{13}^- cluster is 2.86 eV which is larger than that of other anions. The $Al_{13}D_2$ and $Al_{13}D_2^-$ are tested to have enhanced stability according to their binding energies (2.43 and 2.65 eV). The adsorption energies of two D atoms on neutral and anionic Al_{13} are calculated to be 5.37 and 5.48 eV, respectively. These are very small number comparing with the values in Fig. 6.

3.4. HOMO–LUMO gaps

Frontier orbital theory tells us that the highest occupied orbital (HOMO) and the lowest unoccupied molecular orbital (LUMO) play an important role in chemical reactions [64,65]. The energy gap between HOMO and LUMO can represent the ability of molecule to participate into chemical reaction in some degree [66]. A closed electron configuration with a large HOMO–LUMO energy gap is a prerequisite for the chemical stability of a cluster [67]. So we examined the HOMO–LUMO energy gap for the most stable Al_n^{λ}

Table 3
Natural charges populations of the ground-state Al_nD_2 (n = 1–9) clusters. The Al atoms bonding to deuterium atom denoted are in bold.

Isomers	D-1	D-2	Al-1	Al-2	Al-3	Al-4	Al-5	Al-6	Al-7	Al-8	Al-9
AlD_2	−0.415	−0.415	**0.830**								
Al_2D_2	−0.462	−0.462	**0.462**	**0.462**							
Al_3D_2	−0.397	−0.397	**0.411**	**0.411**	−0.028						
Al_4D_2	−0.376	−0.376	**0.385**	−0.265	0.247	**0.385**					
Al_5D_2	−0.348	−0.348	−0.014	−0.014	**0.543**	−0.361	**0.543**				
Al_6D_2	−0.349	−0.349	0.049	**0.120**	0.049	**0.180**	**0.120**	**0.180**			
Al_7D_2	−0.301	−0.325	0.064	**0.257**	−0.026	0.023	−0.021	**0.174**	0.155		
Al_8D_2	−0.335	−0.335	−0.111	0.034	−0.111	0.034	0.183	−0.352	**0.496**	**0.496**	
Al_9D_2	−0.285	−0.285	0.186	0.186	−0.148	−0.148	−0.036	−0.036	**0.166**	**0.166**	0.236

Table 4
Natural charges populations of the ground-state $Al_nD_2^-$ (n = 1–9) clusters. The Al atoms bonding to deuterium atom denoted are in bold.

Isomers	D-1	D-2	Al-1	Al-2	Al-3	Al-4	Al-5	Al-6	Al-7	Al-8	Al-9
AlD_2^-	−0.481	−0.481	**−0.038**								
$Al_2D_2^-$	−0.416	−0.416	**−0.084**	**−0.084**							
$Al_3D_2^-$	−0.407	−0.407	**0.101**	**0.101**	−0.387						
$Al_4D_2^-$	−0.356	−0.356	**0.097**	−0.241	−0.241	**0.097**					
$Al_5D_2^-$	−0.384	−0.384	−0.220	−0.220	**0.412**	−0.615	**0.412**				
$Al_6D_2^-$	−0.181	−0.181	−0.256	**−0.028**	**−0.221**	**−0.028**	−0.142	**0.037**			
$Al_7D_2^-$	−0.357	−0.357	−0.080	**0.209**	−0.271	−0.171	−0.171	**0.209**	−0.013		
$Al_8D_2^-$	−0.329	−0.329	−0.140	0.045	−0.140	**0.176**	−0.253	**0.176**	−0.253	0.045	
$Al_9D_2^-$	−0.314	−0.314	−0.295	**0.149**	−0.010	**0.149**	−0.114	0.077	0.117	−0.223	−0.223

and $Al_nD_2^{\lambda}$ (n = 1–9, 13; λ = 0, −1) clusters. The HOMO, LUMO energies and HOMO–LUMO gaps are listed in Table 2. In addition, the HOMO–LUMO gaps against the cluster size are also plotted in Fig. 7. It is clear from the Table 2 that Al_{13}^- has a particularly large HOMO–LUMO gap (2.73 eV). This may be due to that it possess 40 electrons and can fill the electronic shells. But we think that a cluster with a closed electronic shell is characterized not only by a large HOMO–LUMO gap but also by a filled HOMO. According to Janak's theorem [68], HOMO energy can reflect the ability of molecule to lose electrons in some degree. A high HOMO energy implies negative ionization energy. The anionic Al_2^-, Al_8^- and $Al_2D_2^-$ clusters have positive HOMO energy, which indicate the real system should eject the excess electron spontaneously. As see from Fig. 7, there are no apparent odd–even alternation behaviors in these curves, except for that of Al_n. For pure aluminum clusters, the HOMO–LUMO gaps of Al_5, Al_7, Al_8, Al_2^- and Al_7^- are larger than others; while for adsorbed clusters, the conspicuous peaks appear at Al_2D_2, Al_6D_2, and $Al_7D_2^-$. Those suggest that these clusters possess enhanced chemical stability, which is in accord with the above analysis based on $E_b(n)$, and $\Delta_2(E_n)$. The HOMO–LUMO gaps of $Al_{13}D_2$ and $Al_{13}D_2^-$ are listed in Table 2, and the values are calculated to be 1.35 and 2.75 eV, respectively. Comparing with the pure $Al_{13}^{0/-}$ clusters, the HOMO–LUMO gaps of adsorption clusters have very small changes. This implies that the adsorption of D atoms exert a very small influence on the electronic structure of $Al_{13}^{0/-}$ clusters.

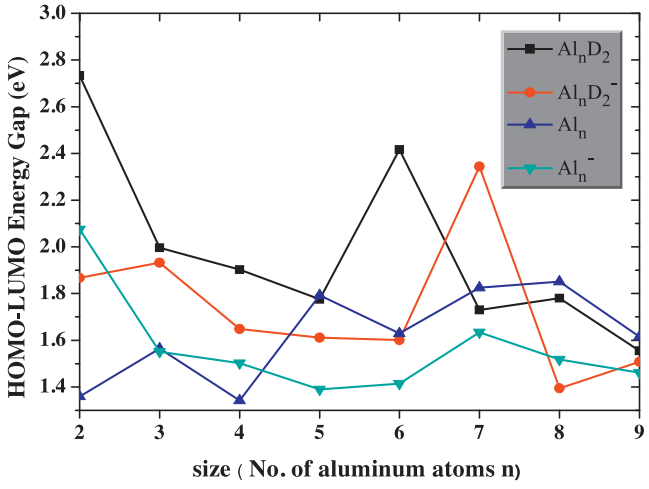

Fig. 7. Size dependence of the HOMO–LUMO energy gaps of ground-state Al_n^{λ} and $Al_nD_2^{\lambda}$ (n = 2–9; λ = 0, −1) clusters.

3.5. Electronic properties

In order to probe into the localization of the charges and reliable charge-transfer information in Al_nD_2 and $Al_nD_2^-$ clusters, the natural population analysis (NPA) for the lowest energy species have been calculated and summarized in Tables 3 and 4. The atom numeration to identify Al atoms is shown in Figs. 2 and 3, respectively. As shown in Table 3, it can be clearly seen that the two deuterium atoms in neutral Al_nD_2 clusters possess the equal negative charges, which are in the range of −0.462 to −0.285e. While the Al atoms direct bonding to deuterium atom possess positive charges. This indicates that the electrons transfer from the Al_n frames to D atoms, namely, deuterium acts as electron accepter in all the neutral clusters. This may be due to the electronegativity of D (2.20) is much larger than Al (1.61); therefore the deuterium has a stronger ability to attract electrons. When a negative charge is added to the clusters, the deuterium atoms possess the negative charges in the range of −0.481 to −0.181e. Comparing with the neutral Al_nD_2 clusters, the charges of deuterium atoms have a little change. Furthermore, we find that the charges on the two deuterium atoms are always equal. This may be due to the fact that the two deuterium atoms are located at the same site in the identical cluster. In other words, the charge distribution depends on the symmetry of cluster. Moreover, in order to show where the charges locate visually, the electron localization function (ELF) was investigated. It shows a clear separation between the core and valence electron, and also shows covalent bonds and lone pairs. The maps for the ground-state structures of $Al_nD_2^{\lambda}$ (n = 2–9; λ = 0, −1) clusters are shown in supplementary material (Fig. S4).

To achieve a deep insight into the redistribution of electron density, the difference electron density has been investigated using the Multiwfn [69,70]. It is the difference between the density of ground state $Al_nD_2^{0/-}$ and the superposition of those corresponding to D

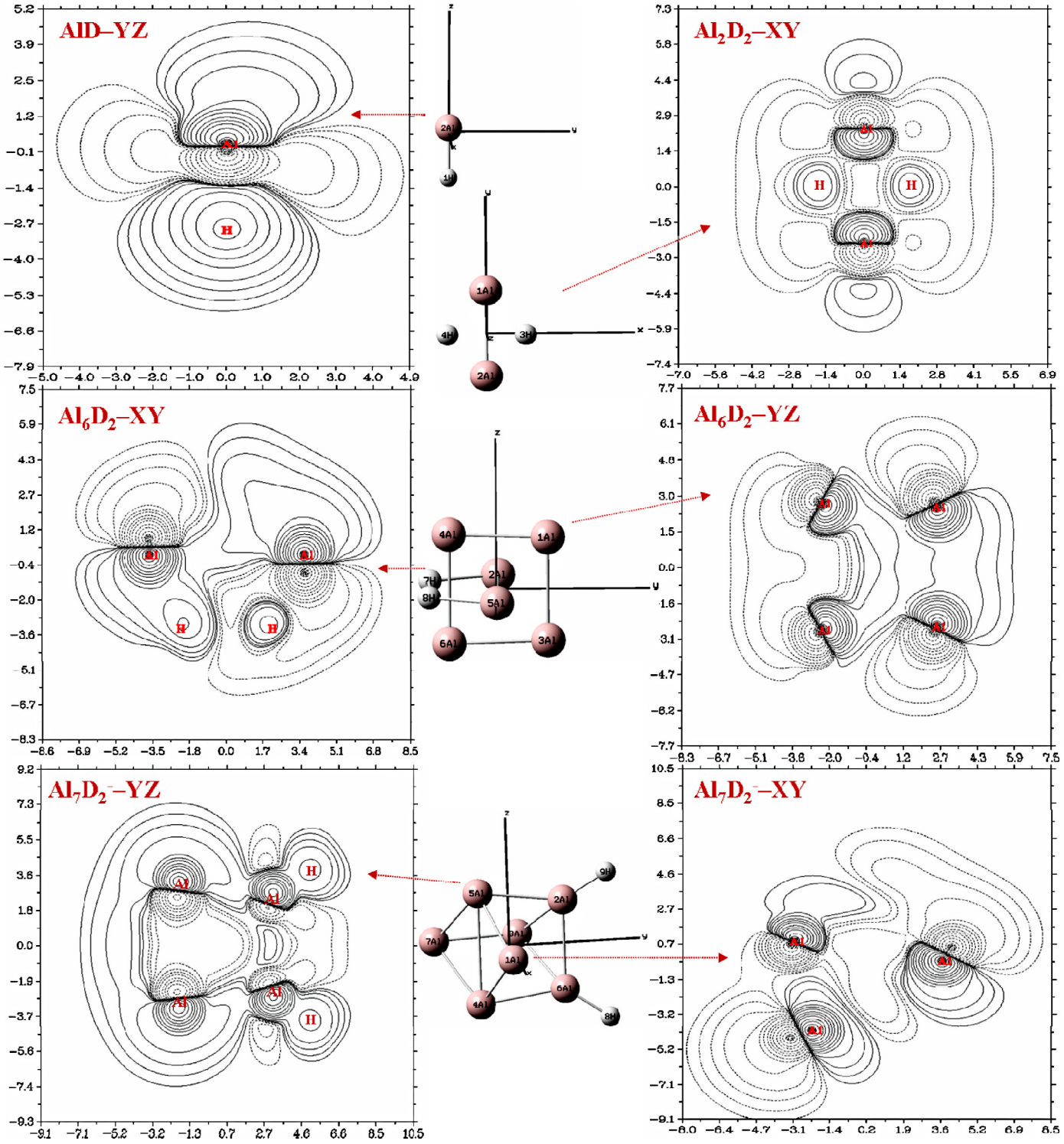

Fig. 8. The difference electron density for the AlD, Al_2D_2, Al_6D_2, and $Al_7D_2^-$ clusters.

atoms and Al_n frames. It can provide qualitative information on the electron flow over the whole cluster upon metal coordination. The maps for the selected clusters (AlD, Al_2D_2, Al_6D_2, and $Al_7D_2^-$) are shown in Fig. 8. As might be seen from these plots, the solid line designate an increase of the electron density ($\Delta\rho > 0$), whereas the dashed line indicate a decrease of the electron density ($\Delta\rho < 0$). The length unit is Bohr. Most of the selected clusters have three-dimensional (3D) structures, while the maps show the difference electron density for a plane. Because our main attention focuses on the electron flow between D and Al atoms, we selected some planes which can reflect the influence of the deuterium atoms. In addition, the geometrical structures in Cartesian coordinates of the selected clusters are also performed for a better view.

It is clear from the maps of AlD dimer that there exists a large density flow from aluminum to deuterium atom upon coordination, which is ascribed to a stronger electron-withdrawing capability of deuterium atom. This is in accord with the natural population analysis, which shows that the Al and D atoms in AlD dimer possess

0.602 and −0.602e charges, respectively. As for Al_2D_2 clusters, the two D atoms adsorbed on the bridge sits of the Al_2 dimer. A lot of electrons which belong to Al atoms are electrostatic attracted by the deuterium nuclei and show apparent polarization. In this case, the electron density of the intermediate region of the two aluminum atoms is significant increase, which can generate the stronger Al—Al and Al—D bond. This can explain why the Al_2D_2 clusters have enhanced stability and the largest adsorption energy. In the case of Al_6D_2 clusters, there are two Al atoms and two D atoms in XY plane, and we can clearly see the direction of electron flow. The four Al atoms in YZ plane correspond to 1Al, 3Al, 4Al and 6Al, respectively. The 4Al and 6Al atoms are obviously affected by the deuterium atoms, therefore the electron density in their left region are reduced. From the YZ plane of $Al_7D_2^-$ cluster, we can clearly see some concentration of electron between D and its closest Al atom. This may indicate a strong covalent component in the bonding.

4. Conclusions

We have performed a systematic investigation on small pure aluminum Al_n^{λ} and aluminum dideuteride $Al_nD_2^{\lambda}$ (n = 1–9, 13; λ = 0, −1) clusters using density functional theory at B3PW91/6-311++G (2d, 2p) level. All the results are summarized as follows.

1. Extensive searches for the ground-state structures were carried out with the aid of comparisons between the simulated spectra and experimental PES data. The results show the ground-state $Al_nD_2^{0/-}$ clusters favor the three-dimensional (3D) structures except for Al_3D_2, Al_5D_2, $Al_3D_2^-$ and $Al_4D_2^-$. The D_2 molecule prefers to dissociate into deuterium atom and then forms the radial Al—D bond with one aluminum atom. Only when n = 2 and 6, the D atoms are edge-capped and face-capped on the aluminum clusters.
2. By calculating the binding energies per atom, second difference energies and HOMO–LUMO gaps, we found the Al_2D_2, Al_6D_2 and $Al_7D_2^-$ clusters have the stronger relative stability and enhanced chemical stability. On the other hand, the adsorption energies of these three clusters are also large. Accordingly, Al_2, Al_6 and Al_7^- may be the better candidates for dissociative adsorption of deuterium molecule among the clusters we have studied.
3. Our natural population analysis (NPA) results indicate that the electrons transfer from the Al_n frames to D atoms in all the neutral clusters. Furthermore, the difference electron density maps, which can provide qualitative information on the redistribution of electron density, are also performed for the selected stable clusters.

Acknowledgments

This work was supported by the National Natural Science Foundation of China (No. 11274235 and No. 11104190), the Doctoral Education Fund of Education Ministry of China (No. 20100181110086 and No. 20110181120112) and Baoji University of Arts and Sciences Key Research Grant (grant no. ZK12048).

Appendix A. Supplementary data

Supplementary material related to this article can be found, in the online version, at http://dx.doi.org/10.1016/j.jmgm.2014.07.016.

References

[1] S.A. Claridge, A.W. Castleman Jr., S.N. Khanna, C.B. Murray, A. Sen, P.S. Weiss, Cluster-assembled materials, ACS Nano 3 (2009) 244–255.
[2] H. Schnöckel, Formation, structure and bonding of metalloid Al and Ga clusters. A challenge for chemical efforts in nanosciences, Dalton Trans. 33 (2008) 4344–4362.
[3] A. Martínez, A. Vela, Stability of charged aluminum clusters, Phys. Rev. B 49 (1994) 17464–17467.
[4] A. Martínez, A. Vela, D.R. Salahub, P. Calaminici, N. Russo, Aluminum clusters. A comparison between all electron and model core potential calculations, J. Chem. Phys. 101 (1994) 10677–10685.
[5] A. Grubisic, X. Li, G. Gantefoer, K.H. Bowen, H. Schnöckel, F.J. Tenorio, A. Martínez, Reactivity of aluminum cluster anions with ammonia: selective etching of Al_{11}^- and Al_{12}^-, J. Chem. Phys. 131 (2009) 184305–184312.
[6] J.N. Li, M. Pu, C.C. Ma, Y. Tian, J. He, D.G. Evans, The effect of palladium clusters (Pd_n, n = 2–8) on mechanisms of acetylene hydrogenation: a DFT study, J. Mol. Catal. A: Chem. 359 (2012) 14–22.
[7] W.A. deHeer, W.D. Knight, M.Y. Chou, M.L. Cohen, Electronic shell structure and metal clusters, Sol. State Phys. 40 (1987) 93–181.
[8] W. Ekardt, Dynamical polarizability of small metal particles: self-consistent spherical jellium background model, Phys. Rev. Lett. 52 (1984) 1925–1928.
[9] B.K. Rao, P. Jena, Evolution of the electronic structure and properties of neutral and charged aluminum clusters: a comprehensive analysis, J. Chem. Phys. 111 (1999) 1890–1904.
[10] R. Ahlrichs, S.D. Elliott, Clusters of aluminium, a density functional study, Phys. Chem. Chem. Phys. 1 (1999) 13–21.
[11] D.M. Cox, D.J. Trevor, R.L. Whetten, A. Kaldor, Aluminum clusters: ionization thresholds and reactivity toward deuterium, water, oxygen, methanol, methane, and carbon monoxide, J. Phys. Chem. 92 (1988) 421–429.
[12] B.K. Rao, P. Jena, Physics of small metal clusters: topology, magnetism, and electronic structure, Phys. Rev. B 32 (1985) 2058–2069.
[13] H. Hakkinen, M. Manninen, How 'magic' is a magic metal cluster? Phys. Rev. Lett. 76 (1996) 1599–1602.
[14] X. Li, H. Wu, X.B. Wang, L.S. Wang, s–p hybridization and electron shell structures in aluminum clusters: a photoelectron spectroscopy study, Phys. Rev. B 81 (1998) 1909–1912.
[15] M.D. Deshpande, D.G. Kanhere, Ab initio absorption spectra of Al_n (n = 2–13) clusters, Phys. Rev. B 68 (2003) 035428–5035432.
[16] W. Lu, J.J. Zhao, Z. Zhou, S.B. Zhang, Z. Chen, First-principles study of molecular hydrogen dissociation on doped $Al_{12}X$ (X = B, Al, C, Si, P, Mg, and Ca) clusters, J. Comput. Chem. 30 (2009) 2509–2514.
[17] M.X. Chen, X.H. Yan, Enhanced stability of Al_7H_3 and Al_7H_7 clusters, Chem. Phys. Lett. 439 (2007) 270–273.
[18] A. Mañanes, F. Duque, F. Méndez, M.J. López, J.A. Alonso, Analysis of the bonding and reactivity of H and the Al_{13} cluster using density functional concepts, J. Chem. Phys. 119 (2003) 5128–5141.
[19] I. Yarovsky, A. Goldberg, DFT study of hydrogen adsorption on Al_{13} clusters, Mol. Simul. 31 (2005) 475–481.
[20] Y.K. Han, J. Jung, K.H. Kim, Structure and stability of $Al_{13}H$ clusters, J. Chem. Phys. 122 (2005) 124319–124323.
[21] J. Jung, Y.K. Han, Structure and stability of $Al_{13}H_n$ (n = 1–13) clusters: exceptional stability of $Al_{13}H_{13}$, J. Chem. Phys. 125 (2006) 064306–064308.
[22] J.E. Fowler, J.M. Ugalde, Al_{12} and the $Al@Al_{12}$ clusters, Phys. Rev. A 58 (1998) 383–388.
[23] K. Gundersen, K.W. Jacobsen, J.K. Nørskov, B. Hammer, The energetics and dynamics of H_2 dissociation on Al(1 1 0), Surf. Sci. 304 (1994) 131–144.
[24] J. Paul, Hydrogen adsorption on Al(1 0 0), Phys. Rev. B 37 (1988) 6164–6174.
[25] T.H. Upton, Structural electronic, and chemisorption properties of small aluminum clusters, Phys. Rev. Lett. 56 (1986) 2168–2171.
[26] T.H. Upton, D.M. Cox, A. Kaldor, in: Jena P. (Ed.), The Physics and Chemistry of Small Clusters, Plenum, New York, 1987.
[27] D.M. Cox, D.J. Trevor, R.L. Whetten, A. Kaldor, Aluminum clusters: ionization thresholds and reactivity toward deuterium, water, oxygen, methanol methane, and carbon monoxide, J. Phys. Chem. 92 (1988) 421–429.
[28] D.J. Henry, A. Varano, I. Yarovsky, Performance of numerical basis set DFT for aluminum clusters, J. Phys. Chem. A 112 (2008) 9835–9844.
[29] A. Varano, D.J. Henry, I. Yarovsky, DFT study of H adsorption on magnesium-doped aluminum clusters, J. Chem. Phys. A 114 (2010) 3602–3608.
[30] D.J. Henry, I. Yarovsky, Dissociative adsorption of hydrogen molecule on aluminum clusters: effect of charge and doping, J. Phys. Chem. A 113 (2009) 2565–2571.
[31] D.J. Henry, A. Varano, I. Yarovsky, First principles investigation of H addition and abstraction reactions on doped aluminum clusters, J. Phys. Chem. A 113 (2009) 5832–5837.
[32] A. Varano, D.J. Henry, I.J. Yarovsky, Role of hydrogen in dimerization of aluminum clusters: a theoretical study, J. Phys. Chem. A 115 (2011) 7734–7743.
[33] L.F. Cui, X. Li, L.S. Wang, Photoelectron spectroscopy of $Al_nD_2^-$ (n = 3–15): observation of chemisorption and physisorption of dideuterium on aluminum cluster anions, J. Chem. Phys. 124 (2006) 054308–054312.
[34] M.J. Frisch, G.W. Trucks, H.B. Schlegel, G.E. Scuseria, M.A. Robb, J.R. Cheeseman, J.A. Montgomery Jr., T. Vreven, K.N. Kudin, J.C. Burant, J.M. Millam, S.S. Iyengar, J. Tomasi, V. Barone, B. Mennucci, M. Cossi, G. Scalmani, N. Rega, G.A. Petersson, H. Nakatsuji, M. Hada, M. Ehara, K. Toyota, R. Fukuda, J. Hasegawa, M. Ishida, T. Nakajima, Y. Honda, O. Kitao, H. Nakai, M. Klene, X. Li, J.E. Knox, H.P. Hratchian, J.B. Cross, V. Bakken, C. Adamo, J. Jaramillo, R. Gomperts, R.E. Stratmann, O. Yazyev, A.J. Austin, R. Cammi, C. Pomelli, J. Ochterski, P.Y. Ayala, K. Morokuma, G.A. Voth, P. Salvador, J.J. Dannenberg, V.G. Zakrzewski, S. Dapprich, A.D. Daniels, M.C. Strain, O. Farkas, D.K. Malick, A.D. Rabuck, K. Raghavachari, J.B. Foresman, J.V. Ortiz, Q. Cui, A.G. Baboul, S. Clifford, J. Cioslowski, B.B. Stefanov,

G. Liu, A. Liashenko, P. Piskorz, I. Komaromi, R.L. Martin, D.J. Fox, T. Keith, M.A. Al-Laham, C.Y. Peng, A. Nanayakkara, M. Challacombe, P.M.W. Gill, B.G. Johnson, W. Chen, M.W. Wong, C. Gonzalez, J.A. Pople, Gaussian 03, Revision C.01, Gaussian, Inc., Wallingford, CT, 2004.
[35] A.D. Becke, Density-functional thermochemistry. III. The role of exact exchange, J. Chem. Phys. 98 (1993) 5648–5652.
[36] J.P. Perdew, in: P. Ziesche, H. Eschrig (Eds.), Electronic Structure of Solids, Akademie Verlag, Berlin, 1991, pp. 11–20.
[37] J.P. Perdew, J.A. Chevary, S.H. Vosko, K.A. Jackson, M.R. Pederson, D.J. Singh, C. Fiolhais, Atoms, molecules, solids, and surfaces: applications of the generalized gradient approximation for exchange and correlation, Phys. Rev. B 46 (1992) 6671–6687.
[38] J.P. Perdew, Y. Wang, Accurate and simple analytic representation of the electron-gas correlation energy, Phys. Rev. B 45 (1992) 13244–13249.
[39] R. Krishnan, J.S. Binkley, R. Seeger, J.A. Pople, Self-consistent molecular. orbital methods. 21. Small split-valence basis sets for first-row elements, J. Am. Chem. Soc. 72 (1980) 650–655.
[40] W.J. Hehre, L. Radom, P.V.R. Schleyer, J.A. Pople, Ab Initio Molecular Orbital Theory, Wiley, New York, 1986.
[41] X. Li, H. Wu, X.B. Wang, L.S. Wang, s–p hybridization and electron shell structures in aluminum clusters: a photoelectron spectroscopy study, Phys. Rev. Lett. 81 (1998) 1909–1912.
[42] K.J. Taylor, C.L. Pettiette, M.J. Graycraft, O. Chesnovsky, R.E. Smalley, Ups of negative aluminum clusters, Chem. Phys. Lett. 152 (1988) 347–352.
[43] J.O. Joswig, M. Springborg, Genetic-algorithms search for global minima of aluminum clusters using a Sutton-Chen potential, Phys. Rev. B 68 (2003) 085408–085416.
[44] J. Sun, W.C. Lu, H. Wang, Z.S. Li, C.C. Sun, Theoretical study of Al_n and Al_nO (n = 2–10) clusters, J. Phys. Chem. A 110 (2006) 2729–2738.
[45] B.K. Rao, P. Jena, Alkalization of aluminum clusters, J. Chem. Phys. 113 (2000) 1508–1513.
[46] R. Fournier, Trends in energies and geometric structures of neutral and charged aluminum clusters, J. Chem. Theory Comput. 3 (2007) 921–929.
[47] X. Yuan, L. Liu, X. Wang, M. Yang, K.A. Jackson, J. Jellinek, Theoretical investigation of adsorption of molecular oxygen on small copper clusters, J. Phys. Chem. A 115 (2011) 8705–8713.
[48] H. Kawamura, V. Kumar, Q. Sun, Y. Kawazoe, Magic behavior and bonding nature in hydrogenated aluminum clusters, Phys. Rev. B 65 (2001) 045406.
[49] H.K. Birnbaum, C. Buckley, F. Zeides, E. Sirois, P. Rozenak, S. Spooner, J.S. Lin, Hydrogen in aluminum, J. Alloy Compd. 253 (1997) 260–264.
[50] B. Kiran, P. Jena, X. Li, A. Grubisic, S.T. Stokes, G.F. Ganteför, K.H. Bowen, R. Burgert, H. Schnöckel, Magic rule for Al_nH_m magic clusters, Phys. Rev. Lett. 98 (2007) 256802–256805.
[51] I. Pino, G.J. Kroes, M.C. van Hemert, Hydrogen dissociation on small aluminum clusters, J. Chem. Phys 133 (2010) 184304–184315.
[52] A. Martínez, F.J. Tenorio, J.V. Ortiz, Electronic structure of Al_3O_n and $Al_3O_n^-$ (n = 1–3) clusters, J. Phys. Chem. A 105 (2001) 8787–8793.
[53] A. Martínez, F.J. Tenorio, J.V. Ortiz, Electronic structure of AlO_2, AlO_2^-, Al_3O_5, and $Al_3O_5^-$ clusters, J. Phys. Chem. A 105 (2001) 11291–11294.
[54] A. Martínez, L.E. Sansores, R. Salcedo, F.J. Tenorio, J.V. Ortiz, Al_3O_n and $Al_3O_n^-$ (n = 1–3) clusters: structures, photoelectron spectra, harmonic vibrational frequencies, and atomic charges, J. Phys. Chem. A 106 (2002) 10630–10635.
[55] A.G. García, A. Martínez, J.V. Ortiz, Addition of water, methanol, and ammonia to $Al_3O_n^-$ clusters: reaction products, transition states, and electron detachment energies, J. Chem. Phys. 122 (2005) 214309–214316.
[56] F.J. Tenorio, I. Murray, A. Martínez, K.J. Klabunde, J.V. Ortiz, Products of the addition of water molecules to Al_3O_3 clusters: structure, bonding, and electron binding energies in $Al_3O_4H_2$, $Al_3O_5H_4$, $Al_3O_3H_2$, and $Al_3O_5H_4$, J. Chem. Phys. 120 (2004) 7955–7962.
[57] A.G. García, A. Martínez, J.V. Ortiz, Are structures with Al–H bonds represented in the photoelectron spectrum of $Al_3O_4H_2$? J. Chem. Phys. 124 (2006) 214304–214308.
[58] C. Lee, W. Yang, R.G. Parr, Development of the Colle-Salvetti correlation-energy formula into a functional of the electron density, Phys. Rev. B 37 (1988) 785–789.
[59] M. Malagoli, V. Coropceanu, D.A. da Silva Filho, J.L. Brédas, A multimode analysis of the gas-phase photoelectron spectra in oligoacenes, J. Chem. Phys. 120 (2004) 7490–7496.
[60] J. Wu, X.Y. Zhang, F. Chen, Z.F. Cui, Ab initio calculations and spectral simulation of the P_2H (X^2A')–P_2H^-(X^1A') photodetachment process, J. Mol. Struct. Thochem. 767 (2006) 149–153.
[61] C.G. Zhan, F. Zheng, D.A. Dixon, Electron affinities of Al_n clusters and multiplefold aromaticity of the square Al_{42}-structure, J. Am. Chem. Soc. 124 (2002) 14795–14803.
[62] A. Varano, D.J. Henry, I. Yarovsky, Role of hydrogen in dimerization of aluminum clusters: a theoretical study, J. Phys. Chem. A 115 (2011) 7734–7743.
[63] C.C. Wang, R.N. Zhao, J.G. Han, Geometries and magnetisms of the Zrn (n = 2–8) clusters: the density functional investigations, J. Chem. Phys. 124 (2006) 194301–194308.
[64] K. Fukui, T. Yonezawa, H. Shingu, A molecule orbital theory of reactivity in aromatic hydrocarbons, J. Chem. Phys. 20 (1952) 722–725.
[65] K. Fukui, Acc. Chem. Res. 4 (1971) 57–64.
[66] J. Aihara, Correlation found between the HOMO–LUMO energy separation and the chemical reactivity at the most reactive site for isolated-pentagon isomers of fullerenes, Phys. Chem. Chem. Phys. 2 (2000) 3121–3125.
[67] J. Li, X. Li, H.J. Zhai, L.S. Wang, Au_{20}: a tetrahedral cluster, Science 181 (2003) 864–867.
[68] J.F. Janak, Proof that $\partial E \partial n_i = \varepsilon$ in density-functional theory, Phys. Rev. B 18 (1978) 7165–7168.
[69] T. Lu, Multiwfn, version 2.1.2. http://multiwfn.codeplex.com/
[70] R.G. Parr, W. Yang, Density functional approach to the frontier-electron theory of chemical reactivity, J. Am. Chem. Soc. 106 (1984) 4049–4050.